Drug Delivery

DOI: 10.1002/anie.200907210

A Tumor-Acidity-Activated Charge-Conversional Nanogel as an Intelligent Vehicle for Promoted Tumoral-Cell Uptake and Drug Delivery**

*Jin-Zhi Du, Tian-Meng Sun, Wen-Jing Song, Juan Wu, and Jun Wang**

Within the last decade, persistent efforts have been made in the development of stimuli-responsive drug-delivery systems for controlled drug release. Typical biological stimuli exploited for triggered drug release include pH[1–4] and temperature differences,[3] redox reactions,[5,6] and enzymes.[7,8] Of these stimuli, pH-responsiveness is one of the most frequently used, as pH values in different tissues and cellular compartments vary. For example, the tumor extracellular environment is more acidic ($pH_e \approx 6.5$) than blood ($pH \approx 7.4$), and the pH values of endosomes and lysosomes are even lower (ca. 5.0–5.5).[9] By utilizing variations in pH values, a number of pH-responsive delivery vehicles, including polymeric micelles,[2,3] nanogels,[10–12] and polymer–drug conjugates,[13,14] have been developed for pH-triggered drug delivery. However, most of them are more sensitive to the significantly acidic endo-/lysosomal conditions than to the slightly acidic tumor extracellular environment. The pursuit of nanocarriers that can be activated by tumor extracellular pH values forms the basis of a new strategy for tumor-targeted drug delivery.[15] The strategy aims to create nanocarriers that maintain their stealth character during circulation and then transform into a more cell-interactive form to display responsive drug release or enhanced interaction between nanocarriers and target cells in a tumor-specific manner. Typical examples are the micellar systems developed by Bae and co-workers that are based on pH_e-responsive poly(L-histidine)-containing block copolymers. These systems expose biotin or TAT peptide on the micelle surface at pH_e values, which leads to enhanced cellular uptake by tumor cells.[16–18] A similar strategy was also described for a TAT-peptide-based liposome system.[19]

Recently, pH-dependent charge conversion was utilized for nanocarrier development for drug delivery. Kataoka and co-workers designed several nanocarriers that were negatively charged under neutral conditions and positively charged at endosomal pH values. Those smart carriers have been used for endosomolytic and lysosomolytic pH-responsive protein and gene delivery.[20–22] Shen and co-workers have also used charge-reversal polymeric micelles[23] and conjugates[24] for nuclear drug delivery, whereby the latter carriers, which were decorated with folic acid, displayed superior cell-killing efficiency. However, nanocarriers with tumor-activated charge-conversional features for enhanced cellular uptake remain scarcely investigated. It has been reported that the surface charge of the nanoparticles plays an important role in their fate, both in vitro and in vivo.[25] Positively charged nanoparticles show higher affinity for negatively charged cell membranes and thus can be readily internalized by the cells, as proved by many investigations.[26,27] However, positively charged nanoparticles always interact strongly with serum components, which causes severe aggregation and rapid clearance from circulation and limits their in vivo application.[28] In contrast, negatively charged carriers have shown potential for protein resistance.[21] Some have exhibited prolonged circulation time for in vivo applications.[26,27]

In this study, we designed a charge-conversional nanogel triggered by pH_e values for enhanced cellular internalization both in vitro and in vivo. We modified an amino-functionalized nanogel with 2,3-dimethylmaleic anhydride (DMMA), which reacted with the amino group to produce an amide bond and a carboxylic acid group. The resultant amide bond is relatively stable at neutral and alkali pH values, but degrades promptly under slightly acidic conditions to expose positively charged amino groups again.[29] The DMMA-modified nanogel was expected to be relatively inert to tumor cells at physiological pH values and to possess high drug-loading efficiency (e.g. of positively charged doxorubicin hydrochloride) owing to the presence of negatively charged carboxylate groups. Once accumulated at the tumor site through the enhanced permeation and retention (EPR) effect,[30] the modified nanogel should be activated to be positively charged in response to the pH_e value. Accordingly, cellular internalization should be enhanced as a result of the strengthened

[*] J.-Z. Du,[+] J. Wu
Department of Polymer Science and Engineering and
CAS Key Laboratory of Soft Matter Chemistry
University of Science and Technology of China
Hefei, Anhui 230026 (China)
T.-M. Sun,[+] W.-J. Song, Prof. J. Wang
Hefei National Laboratory for Physical Sciences at the Microscale
and School of Life Sciences
University of Science and Technology of China
Hefei, Anhui 230027 (China)
Fax: (+86) 551-360-0402
E-mail: jwang699@ustc.edu.cn
[+] These authors contributed equally.

[**] This research was supported by the National Basic Research Program of China (973 Program 2010CB934000, 2009CB930300), the National Natural Science Foundation of China (20974105, 50733003), and the Key Laboratory of Macromolecular Synthesis and Functionalization of the Ministry of Education, Zhejiang University (2009MSF01).

Supporting information for this article is available on the WWW under http://dx.doi.org/10.1002/anie.200907210.

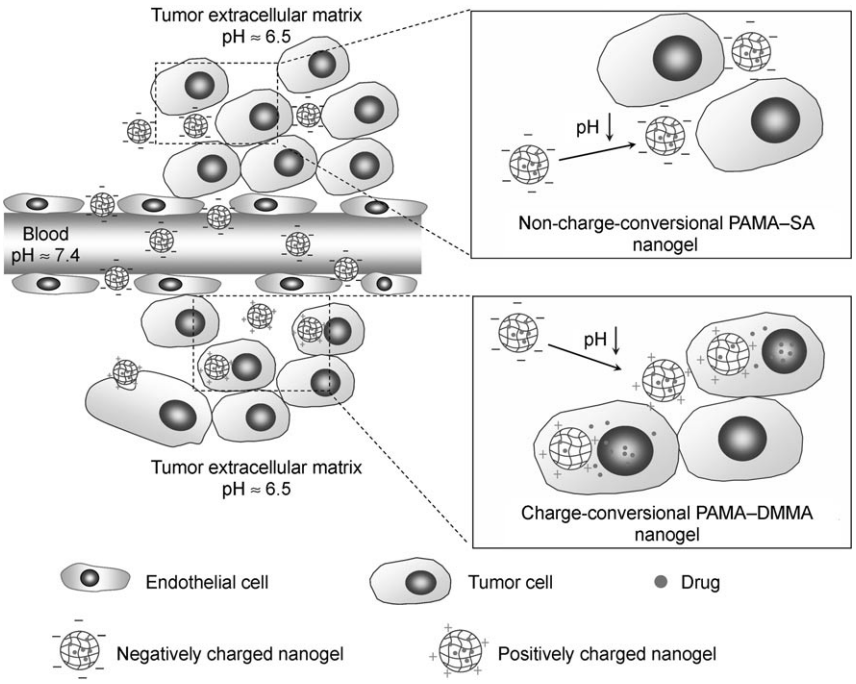

Figure 1. Schematic illustration of the performance of the drug-loaded pH-responsive charge-conversional PAMA–DMMA nanogel and non-charge-conversional PAMA–SA nanogel. During circulation in the blood, the negatively charged PAMA–DMMA and PAMA–SA nanogels both show stealth properties and can leak into tumor sites owing to the EPR effect. In the acidic tumor extracellular environment, the PAMA–DMMA nanogel is activated to be positively charged and is thus readily internalized by tumor cells with subsequent intracellular drug release. In contrast, the non-charge-conversional PAMA–SA nanogel shows relatively weak interaction with tumor cells owing to repulsion between the nanogel and the negatively charged cell membrane.

nanogel–cell interaction to promote intracellular cargo release (Figure 1).

The parent nanogel, poly(2-aminoethyl methacrylate hydrochloride) (PAMA), was prepared by inverse microemulsion polymerization in a hexane/water system with poly(ethylene glycol) diacrylate (PEGDA) as the cross-linker and potassium persulfate as an initiator. Tween-80 and Span-80 were used as surfactants, and the reaction was carried out at 60 °C for 2 h. A PEG content of 9.0 wt % was calculated for the PAMA nanogel from the ^{1}H NMR spectrum. The freeze-dried PAMA nanogel could be readily resuspended in water; it exhibited a positive zeta potential (+30 mV) and unimodal size distribution with a mean particle diameter of approximately 100 nm, as determined by dynamic light scattering (DLS). Furthermore, the nanogel preserved its original state in solvents such as methanol, dimethyl sulfoxide, and acetic acid, which implied that it had a cross-linked rather than an aggregated structure (see the Supporting Information). Subsequently, the nanogel was treated with DMMA to produce a negatively charged nanogel denoted herein as PAMA–DMMA. It was estimated from the integration ratio of the peaks at $\delta = 1.82$ and 0.82–1.00 ppm in the ^{1}H NMR spectrum that approximately 63 % of the amino groups of the PAMA nanogel had been converted into carboxylate groups. The PAMA–DMMA nanogel exhibited significant negative charge, with a zeta potential of −17 mV, and showed relatively uniform morphology, with a particle diameter of approximately 90 nm, as determined by atomic force microscopy (AFM; Figure 2a). The diameter found by AFM was slightly smaller than the result of 122 nm determined by DLS (Figure 2b). For comparison, we prepared a PAMA–SA nanogel by treating the PAMA nanogel with succinic anhydride (SA). PAMA–SA showed a similar particle diameter to that of PAMA–DMMA but had a more negative zeta potential (−25 mV), since more amino groups (75 %) of the PAMA nanogel were converted into carboxylate groups (according to ^{1}H NMR spectroscopic analysis). The chemical structures of the PAMA, PAMA–DMMA, and PAMA–SA nanogels are shown in the Supporting Information.

A key feature of the PAMA–DMMA nanogel is negative-to-positive charge conversion upon exposure to an acidic environment. The charge-conversional behavior of the nanogel was monitored on the basis of the change in zeta potential after incubation at pH 7.4 and 6.8. The zeta potential of the PAMA–DMMA nanogel increased significantly at pH 6.8; it reached 0 mV within 35 min and increased further with a prolonged incubation time (Figure 2c). The zeta potential also increased at pH 7.4, but at a relatively slow rate. In contrast, the zeta potential of the PAMA–SA nanogel remained at around −25 mV at both pH 7.4 and pH 6.8: no sign of charge-conversional behavior was observed (see the Supporting Information). The charge conversion of PAMA–DMMA at pH 6.8 was also confirmed by ^{1}H NMR spectroscopic analysis (Figure 2d). Upon hydrolysis, the intensity of the proton resonance of the PEG methylene hydrogen atoms (H^c) remained constant, whereas the proton resonance of the methylene hydrogen atoms adjacent to the amide (H^a) decreased in intensity and that of the methylene hydrogen atoms adjacent to the amine (H^b) increased in intensity. According to the relative intensity of resonances H^a and H^b, more than 60 % of the amide bonds had been hydrolyzed after 30 min.

Previous studies have shown that positively charged nanoparticles are more readily internalized by cells than negatively charged nanoparticles.[25,27] We used confocal laser scanning microscopy (CLSM) and fluorescence-activated cell sorting (FACS) to investigate the internalization behavior of the nanogel at pH 7.4 and 6.8. Significantly different cellular distribution was observed for the PAMA–DMMA nanogel at different pH values (Figure 3a,b). At pH 6.8, the green fluorescent nanogel was internalized to a remarkable extent and distributed extensively in the cytoplasm, whereas at pH 7.4, the nanogel seemed to be mainly attached to the cell membrane. This difference is probably a result of the PAMA–

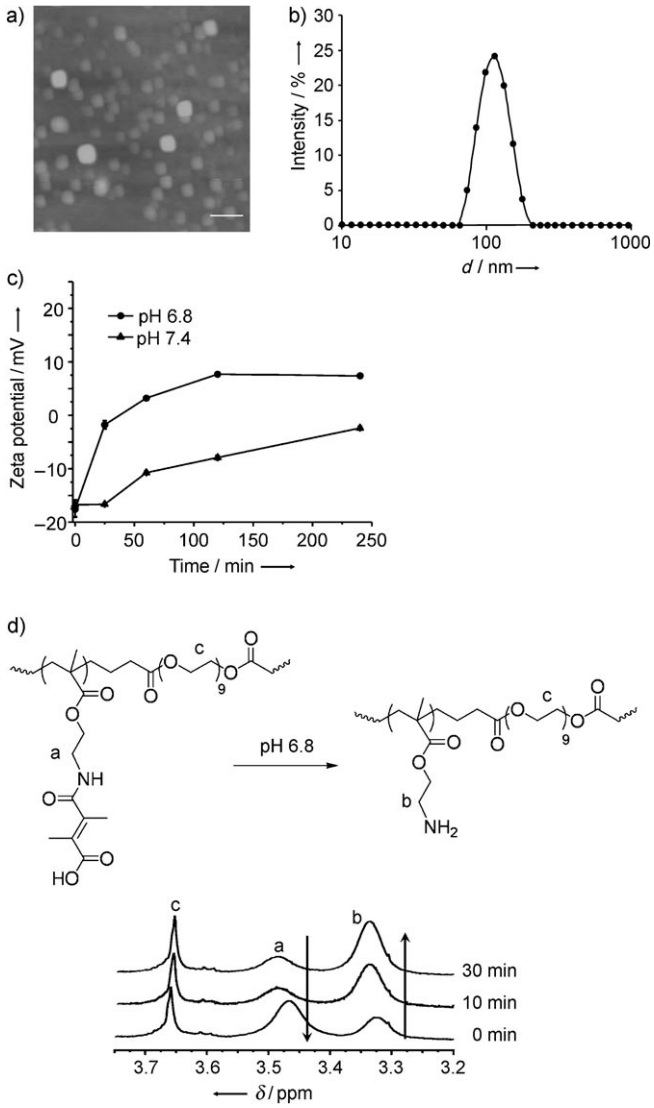

Figure 2. a) AFM image of the PAMA–DMMA nanogel (scale bar: 250 nm). b) Size distribution of the PAMA–DMMA nanogel, as determined by DLS analysis. c) Change in the zeta potential of the PAMA–DMMA nanogel as a function of incubation time at pH 6.8 and 7.4. d) Hydrolysis of PAMA–DMMA at pH 6.8, as monitored by ^{1}H NMR spectroscopy in D_2O/DCl.

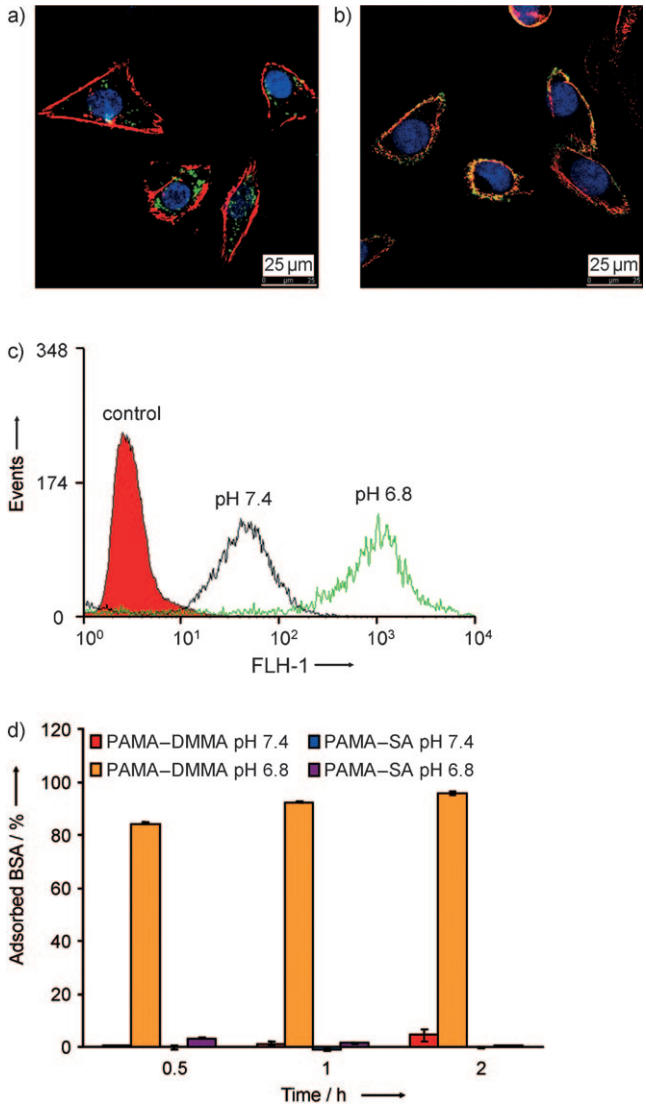

Figure 3. a,b) CLSM images of MDA-MB-435s cells incubated with the PAMA–DMMA nanogel at pH 6.8 (a) and pH 7.4 (b) for 2 h. PAMA–DMMA was labeled with fluorescein isothiocyanate (FITC; green); the F-actin and nuclei of the cells were stained with rhodamine phalloidin (red) and 4′,6-diamidino-2-phenylindole (DAPI; blue), respectively. c) Comparison of cellular uptake of FITC-labeled PAMA–DMMA at pH 7.4 and 6.8 by flow cytometry. FLH-1 represents the fluorescence of FITC. d) BSA adsorption on the nanogels after incubation at 37 °C for different periods of time.

DMMA nanogel becoming positively charged upon hydrolysis at pH 6.8, which strengthens the interaction of the nanogel with cells and enhances cellular internalization. In contrast, the nanogel remains negatively charged at pH 7.4, and cellular internalization is hampered to some extent. This phenomenon was confirmed when the non-charge-conversional PAMA–SA nanogel was incubated with the cells. At both pH 7.4 and pH 6.8, the PAMA–SA nanogel mainly adhered to the cell membrane, and little internalization occurred (see the Supporting Information). Each CLSM image was taken under the individual optimal conditions. The actual intensity of green fluorescence for PAMA–DMMA at pH 6.8 was much higher than that at pH 7.4, which indicates that more of the nanogel was internalized at pH 6.8. This observation was further confirmed by FACS analysis (Figure 3c). Compared with the cellular uptake at pH 7.4, remarkably enhanced intracellular fluorescence was detected at pH 6.8. Thus, charge conversion indeed facilitated the cellular uptake of the nanogel. In contrast, no difference was observed at pH 7.4 and 6.8 by FACS analysis when the non-charge-conversional PAMA–SA nanogel was incubated with the cells (see the Supporting Information).

We also addressed the interaction of the PAMA–DMMA nanogel with proteins to examine the potential of PAMA–DMMA for in vivo applications. We used bovine serum albumin (BSA) as a model protein and PAMA–SA as a control. The PAMA–DMMA nanogel interacted strongly with BSA at pH 6.8: more than 80% BSA adsorption was

observed within only 0.5 h, and absorption increased further with time (Figure 3d). In contrast, at pH 7.4 the nanogel showed very limited BSA adsorption even after incubation for 2 h. Under the same conditions, the PAMA–SA nanogel showed negligible BSA adsorption at both pH values. The results are in agreement with the pH-dependent charge-conversional behavior of the PAMA–DMMA nanogel: at pH 6.8, the PAMA–DMMA nanogel gradually became positively charged and showed increased interaction with the protein BSA, but at pH 7.4 it remained negatively charged and showed protein-resistance characteristics. As the nanogel is protein-resistant at the physiological pH value of 7.4 and shows enhanced interaction with cells and proteins at the tumor pH value of 6.8, it can be considered as an extracellularly activated nanocarrier.

Positively charged doxorubicin hydrochloride (DOX) was used to investigate the drug-loading capacity of the PAMA–DMMA nanogel. The drug was loaded by simply mixing separate aqueous solutions of PAMA–DMMA and DOX at pH 7.4. The PAMA–SA and positively charged parent PAMA nanogels were used as controls. Both negatively charged PAMA–DMMA and PAMA–SA showed extremely high drug-loading efficiency (DLE; 94.9% for PAMA–DMMA and 98.7% for PAMA–SA) relative to that of the PAMA nanogel (18.6%) under the same conditions (see the Supporting Information). This high efficiency may be a result of the interaction of negatively charged PAMA–DMMA or PAMA–SA with positively charged DOX. Indeed, the zeta potential of the nanogel increased upon DOX loading owing to partial neutralization of the carboxylate groups through DOX binding. In contrast, the repulsive force between the PAMA nanogel and DOX may hamper drug loading.

We investigated the in vitro DOX-release behavior of the DOX-loaded PAMA–DMMA nanogel at different pH values. DOX release from the nanogel was pH-dependent: the release rate increased as the pH value decreased (pH 5.5 > pH 6.8 > pH 7.4; Figure 4). A similar trend was observed when the DOX-loaded PAMA–SA nanogel was used (see the Supporting Information). The accelerated DOX release at acidic pH values was probably the result of a decrease in the interaction between the nanogel and DOX upon protonation of the carboxylic acid groups of the nanogel. Such a phenomenon was also observed by Kim et al. upon the release of DOX from polymeric micelles with a cross-linked polyanion core.[31] The PAMA–DMMA and PAMA–SA nanogels showed almost the same final cumulative release at pH 7.4 after reaching the plateau phase (56% for PAMA–DMMA and 54% for PAMA–SA); however, a significantly greater total release from the PAMA–DMMA nanogel (75%) at pH 6.8 was observed than that from PAMA–SA (63%). Given the charge-coversional character of the PAMA–DMMA nanogel at pH 6.8, the enhanced repulsive force between positively charged DOX and the resultant positively charged nanogel should contribute to the increase in total release. Both the PAMA–DMMA and PAMA–SA nanogels displayed relatively severe burst release, which might indicate that the electrostatic interaction between DOX and the nanogel is sensitive to the environmental pH value and the small electrolyte molecules in the buffer.[31] Although the burst drug release from nanogel may not be ideal for application of the nanogel, it can be overcome by the conjugation of drug molecules to the nanogel through an acid-labile bond.[14]

To verify the feasibility of the charge-conversional nanogel for cancer therapy, we tested cell-proliferation inhibition in vitro. MDA-MB-435s cells were incubated with different DOX formulations in Dulbecco modified Eagle medium (DMEM) at pH 7.4 and 6.8 and subjected to an MTT assay (MTT = 3-(4,5-dimethylthiazol-2-yl)-2,5-diphenyltehttp://en.wikipedia.org/wiki/Phenyltrazolium bromide). The DOX-loaded PAMA–DMMA nanogel showed significantly enhanced cell-proliferation inhibition at pH 6.8 relative to that at pH 7.4 ($p < 0.005$), with 57 and 30% cell viability at pH 7.4 and 6.8, respectively, and showed even higher cytotoxicity than free DOX at pH 6.8 (Figure 5). Under acidic conditions, both the cellular uptake of the DOX-loaded charge-conversional PAMA–DMMA nanogel and DOX release are probably enhanced. A slight increase in the cytotoxicity of the DOX-loaded PAMA–SA nanogel was observed under acidic conditions relative to that at pH 7,4, possibly as a result of slightly enhanced DOX release. No

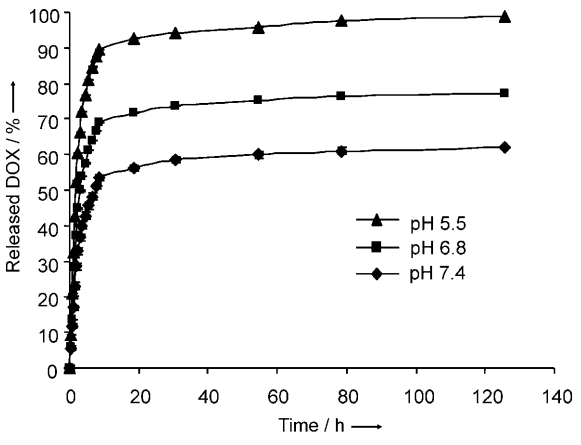

Figure 4. Cumulative DOX release from the PAMA–DMMA nanogel at different pH values. Error bars indicate the standard deviation.

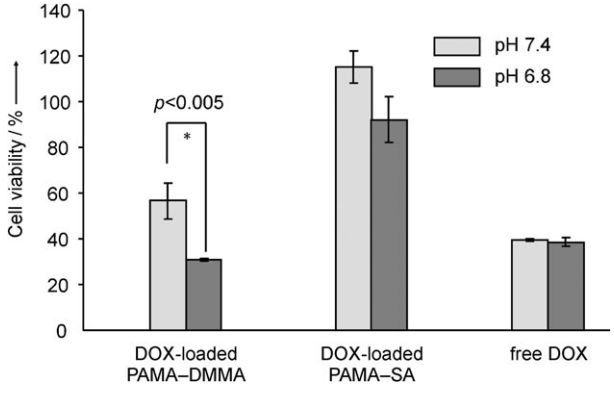

Figure 5. Cell viability of MDA-MB-435s cells after incubation with DOX-loaded PAMA–DMMA, DOX-loaded PAMA–SA, and free DOX at the same DOX concentration of 16 μg mL^{-1}. Data are presented as the average ± standard deviation ($n = 3$); *$p < 0.005$, as determined by the Student's *t*-test.

cytotoxicity difference for free DOX was observed between the experiments at pH 7.4 and 6.8; thus, slightly acidic conditions did not affect the toxicity of DOX. In fact, the use of more acidic conditions (e.g. pH 5.5) was found previously to have no influence on the function of DOX.[32] PAMA–DMMA and PAMA–SA nanogels that were not loaded with DOX did not show cytotoxicity under the same conditions up to a concentration of 100 $\mu g\,mL^{-1}$ (see the Supporting Information).

To further explore the potential of charge-conversional PAMA–DMMA for in vivo cancer therapy, we injected the FITC-labeled nanogel intratumorly into tumor-bearing Balb/c-nu mice and examined its tumoral distribution by CLSM with the FITC-labeled PAMA–SA nanogel as a control. Both the PAMA–DMMA and PAMA–SA nanogels could be detected as green dots in the tumor tissue, but their distribution was remarkably different (Figure 6). As indicated by the white arrows in Figure 6a, most of the PAMA–DMMA nanogel was located in the cytoplasm of tumor cells, whereas the PAMA–SA nanogel remained mainly in the extracellular space or adhered to the cell membrane (Figure 6b). Thus, the charge-conversional PAMA–DMMA nanogel can be internalized more efficiently by tumor cells as a result of the slightly acidic tumor extracellular environment.

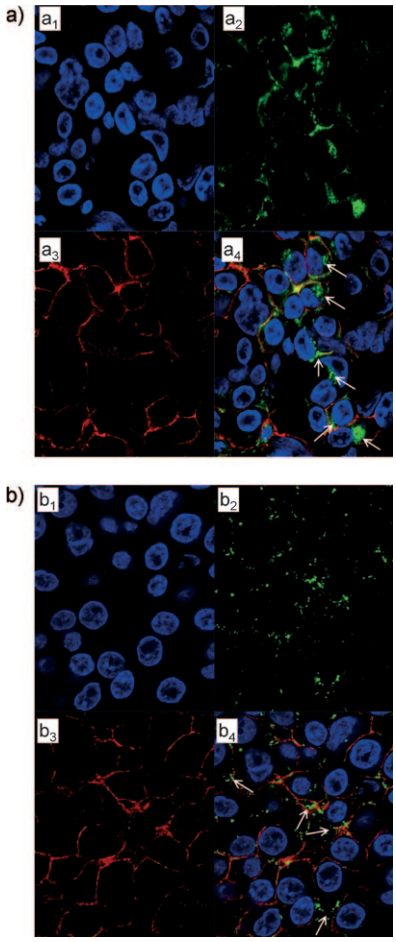

Figure 6. Distribution of FITC-labeled a) PAMA–DMMA and b) PAMA–SA nanogels in tumor tissue following intratumoral injection. a_1 and b_1: DAPI-stained nuclei (blue); a_2 and b_2: FITC-labeled nanogel (green); a_3 and b_3: rhodamine phalloidin labeled F-actin (red); a_4 and b_4: merged images. The white arrows show the location of the nanogels.

In summary, we have developed a pH-responsive charge-conversional nanogel for promoted tumoral-cell uptake and DOX delivery. The nanogel is transformed from a negatively charged form into a positively charged form in the slightly acidic tumor extracellular environment. This charge conversion enhanced the cellular uptake of the nanogel and promoted cargo release, which led to remarkably enhanced efficiency in killing cancer cells. Furthermore, the PAMA–DMMA nanogel is capable of decreased protein absorption under neutral conditions and strong interaction with proteins under slightly acidic conditions. These properties indicate that the creation of nanocarriers with pH_e-responsive charge-conversional properties can be applied to the design of advanced drug carriers for intelligent drug delivery.

Received: December 22, 2009
Revised: March 8, 2010
Published online: April 13, 2010

Keywords: antitumor agents · charge conversion · drug delivery · nanoparticles · pH-responsive

[1] V. Torchilin, *Eur. J. Pharm. Biopharm.* **2009**, *71*, 431.
[2] Y. Bae, K. Kataoka, *Adv. Drug Delivery Rev.* **2009**, *61*, 768.
[3] S. Ganta, H. Devalapally, A. Shahiwala, M. Amiji, *J. Controlled Release* **2008**, *126*, 187.
[4] E. S. Lee, Z. G. Gao, Y. H. Bae, *J. Controlled Release* **2008**, *132*, 164.
[5] R. A. Petros, P. A. Ropp, J. M. DeSimone, *J. Am. Chem. Soc.* **2008**, *130*, 5008.
[6] Y. L. Li, L. Zhu, Z. Liu, R. Cheng, F. Meng, J. H. Cui, S. J. Ji, Z. Zhong, *Angew. Chem.* **2009**, *121*, 10098; *Angew. Chem. Int. Ed.* **2009**, *48*, 9914.
[7] P. D. Thornton, R. J. Mart, R. V. Ulijn, *Adv. Mater.* **2007**, *19*, 1252.
[8] B. Law, C. H. Tung, *Bioconjugate Chem.* **2009**, *20*, 1683.
[9] E. S. Lee, K. T. Oh, D. Kim, Y. S. Youn, Y. H. Bae, *J. Controlled Release* **2007**, *123*, 19.
[10] J. K. Oh, R. Drumright, D. J. Siegwart, K. Matyjaszewski, *Prog. Polym. Sci.* **2008**, *33*, 448.
[11] E. S. Lee, D. Kim, Y. S. Youn, K. T. Oh, Y. H. Bae, *Angew. Chem.* **2008**, *120*, 2452; *Angew. Chem. Int. Ed.* **2008**, *47*, 2418.
[12] A. V. Kabanov, S. V. Vinogradov, *Angew. Chem.* **2009**, *121*, 5524; *Angew. Chem. Int. Ed.* **2009**, *48*, 5418.
[13] Y. Bae, S. Fukushima, A. Harada, K. Kataoka, *Angew. Chem.* **2003**, *115*, 4788; *Angew. Chem. Int. Ed.* **2003**, *42*, 4640.
[14] R. Duncan, *Nat. Rev. Cancer* **2006**, *6*, 688.
[15] E. Gullotti, Y. Yeo, *Mol. Pharm.* **2009**, *6*, 1041.
[16] V. A. Sethuraman, Y. H. Bae, *J. Controlled Release* **2007**, *118*, 216.
[17] E. S. Lee, K. Na, Y. H. Bae, *Nano Lett.* **2005**, *5*, 325.
[18] E. S. Lee, Z. G. Gao, D. Kim, K. Park, I. C. Kwon, Y. H. Bae, *J. Controlled Release* **2008**, *129*, 228.
[19] R. M. Sawant, J. P. Hurley, S. Salmaso, A. Kale, E. Tolcheva, T. S. Levchenko, V. P. Torchilin, *Bioconjugate Chem.* **2006**, *17*, 943.
[20] Y. Lee, S. Fukushima, Y. Bae, S. Hiki, T. Ishii, K. Kataoka, *J. Am. Chem. Soc.* **2007**, *129*, 5362.
[21] Y. Lee, K. Miyata, M. Oba, T. Ishii, S. Fukushima, M. Han, H. Koyama, N. Nishiyama, K. Kataoka, *Angew. Chem.* **2008**, *120*, 5241; *Angew. Chem. Int. Ed.* **2008**, *47*, 5163.

[22] Y. Lee, T. Ishii, H. Cabral, H. J. Kim, J. H. Seo, N. Nishiyama, H. Oshima, K. Osada, K. Kataoka, *Angew. Chem.* **2009**, *121*, 5413; *Angew. Chem. Int. Ed.* **2009**, *48*, 5309.
[23] P. Xu, E. A. Van Kirk, Y. Zhan, W. J. Murdoch, M. Radosz, Y. Shen, *Angew. Chem.* **2007**, *119*, 5087; *Angew. Chem. Int. Ed.* **2007**, *46*, 4999.
[24] Z. Zhou, Y. Shen, J. Tang, M. Fan, E. A. Van Kirk, W. J. Murdoch, M. Radosz, *Adv. Funct. Mater.* **2009**, *19*, 3580.
[25] V. Mailander, K. Landfester, *Biomacromolecules* **2009**, *10*, 2379.
[26] S. E. Gratton, P. A. Ropp, P. D. Pohlhaus, J. C. Luft, V. J. Madden, M. E. Napier, J. M. DeSimone, *Proc. Natl. Acad. Sci. USA* **2008**, *105*, 11613.
[27] E. C. Cho, J. Xie, P. A. Wurm, Y. Xia, *Nano Lett.* **2009**, *9*, 1080.
[28] D. Oupicky, M. Ogris, K. A. Howard, P. R. Dash, K. Ulbrich, L. W. Seymour, *Mol. Ther.* **2002**, *5*, 463.
[29] M. Meyer, A. Philipp, R. Oskuee, C. Schmidt, E. Wagner, *J. Am. Chem. Soc.* **2008**, *130*, 3272.
[30] T. Matsumura, H. Maeda, *Cancer Res.* **1986**, *46*, 6387.
[31] J. O. Kim, A. V. Kabanov, T. K. Bronich, *J. Controlled Release* **2009**, *138*, 197.
[32] D. Kim, E. S. Lee, K. T. Oh, Z. G. Gao, Y. H. Bae, *Small* **2008**, *4*, 2043.

